Design for Gusset Plate Buckling with Variable Stress Trajectories

BO DOWSWELL

ABSTRACT

Gusset plates are used in steel buildings and bridges to connect diagonal members to other framing members in the structural system. Gusset plates subjected to compression loads are currently modeled as rectangular columns with an effective cross section defined by a 30° stress trajectory known as the Whitmore section. The buckling strength is calculated using the AISC column curve with empirical effective length factors. Previous research has shown local yielding allows the stresses to redistribute, increasing the effective width. Because the inelastic capacity decreases with gusset slenderness, a variable stress trajectory has been established which is dependent on the flexural buckling slenderness parameter. This paper describes a design method for the buckling strength of gusset plates using variable stress trajectory angles. The proposed effective length factors for the equivalent column were evaluated using data from existing research. The design model is valid for single- and double-plane corner gusset plates, including extended corner gusset plates commonly used for seismic design. Compared to the results of 162 specimens from 12 previously published research projects, the proposed design model is shown to be more accurate than the methods that are currently available.

Keywords: Gusset plate buckling, stress trajectory, AISC column curve.

INTRODUCTION

Figure 1(a) shows a typical vertical brace connection at a beam-to-column intersection, also known as a corner gusset plate connection. The gusset plate transfers axial load from the brace and distributes it to the beam and column. Figure 1(b) shows a double-plane truss connection that transfers axial load from the diagonal web member to the chord and the vertical web member. Double-plane gusset plates are commonly used to connect wide-flange truss members in long-span trusses. This configuration uses two side-by-side gussets connecting to each flange of the web and chord members.

In practice, gusset plates are treated as rectangular, axially loaded members with a cross section $L_w \times t$, where L_w is the effective width and t is the gusset plate thickness. The effective width is generally calculated with a constant 30° trajectory angle, as shown in Figure 2(a), which was based on the experimental stress trajectories in elastic gusset plates. In this case, the equivalent cross section is known as the Whitmore section (Whitmore, 1952).

Based on a proposal by Thornton (1984), gusset plates in compression are currently designed as rectangular columns with a cross section defined by the Whitmore section. The buckling strength is calculated with the column curve in AISC *Specification* Section E3 (AISC, 2016). For corner gusset plates, the column length, l_{avg}, is the average of l_1, l_2, and l_3 as shown in Figure 2(b).

AISC *Specification* Section E3 for flexural buckling was developed for designing main structural members with various cross-sectional shapes and residual stress patterns. Because connection elements have lower residual stresses and higher shape factors than main members, the buckling strength in the inelastic range is higher than predicted by the AISC *Specification* equations (Dowswell, 2016). To account for this behavior at low slenderness ratios in AISC *Specification* Section J4.4, the critical stress is equal to the specified minimum yield strength when the slenderness ratio is equal to or less than 25.

Effective lengths, $L_c = KL$, have been developed for several common gusset plate geometries. In most cases, the effective length recommendations were calibrated for use with a 30° trajectory angle; therefore, gusset plates are typically designed using an equivalent cross section defined by the Whitmore criterion. The equivalent column method is discussed further in AISC Design Guide 29, *Vertical Bracing Connections—Analysis and Design*, Appendix C (Muir and Thornton, 2014).

Dowswell (2006) summarized the available research on gusset plate stability and proposed effective length factors for various configurations. He also discussed several sources of inaccuracy in the design model, two of which are listed here:

1. Although the effective width is calculated at the last fastener near the end of the brace, the stress continues to spread out beyond the effective width.

Bo Dowswell, PhD, PE, ARC International, LLC, Birmingham, AL. Email: bo@arcstructural.com

Paper No. 2017-17R

2. Due to stress redistribution when the plate yields, the effective width in the inelastic range is larger than predicted using the 30° angle.

In an effort to develop a more accurate design model for gusset plates in compression, these issues are evaluated in this paper. A new design procedure, based on Thornton's equivalent column concept, has been developed. To evaluate the proposed design procedure, the available experimental and finite element results are compared to the predicted strength of each specimen.

Gusset plates are fabricated in many different configurations; however, only two are addressed in this paper: corner gusset plates and extended corner gusset plates. The corner and extended corner configurations have a single brace framing to the gusset plate at the intersection of two other orthogonal framing members. The gusset plate is connected to both members. For corner gussets, a line through the innermost bolts, perpendicular to the brace line of action, intersects one or both of the connected gusset boundaries as shown in Figure 3(a). For the extended corner configuration, the gusset plate is shaped so the free edges are cut at an angle to the connected edges as shown in Figure 3(b). In this case, a line through the innermost bolts, perpendicular to the brace line of action, intersects both of the gusset-free edges.

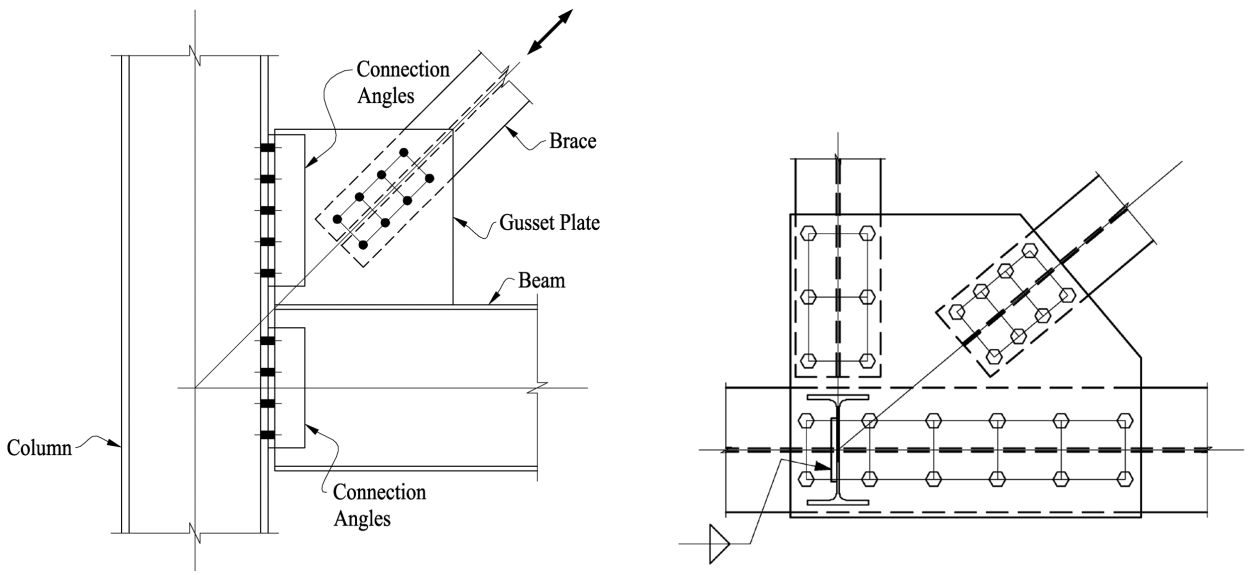

(a) vertical brace connection with a single-plane gusset plate *(b) truss connection with a double-plane gusset plate*

Fig. 1. Gusset plate connections.

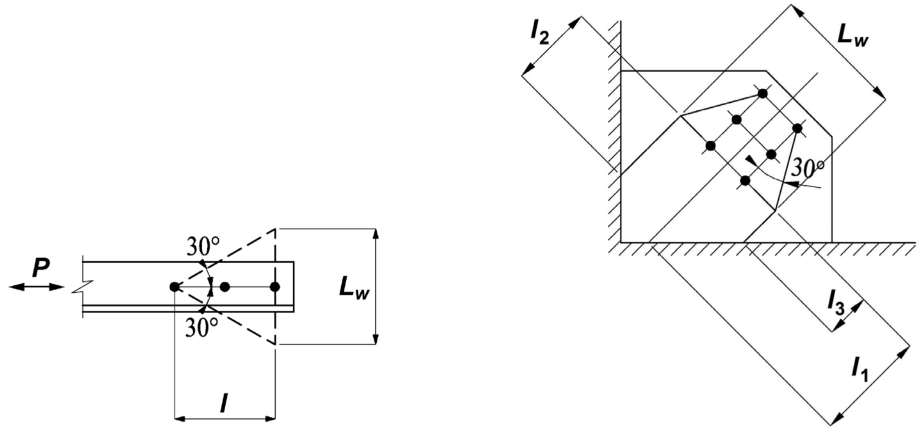

(a) effective width *(b) buckling length*

Fig. 2. Current design of gusset plates.

EXISTING RESEARCH

The existing research on stress trajectories was reviewed by Dowswell (2013). The early research by Wyss (1923), Sandel (1950), and Whitmore (1952) focused on the measurement of elastic stresses. The researchers generally agreed that the stress trajectories formed approximately 30° lines with the connected member. Additional research by Lavis (1967), Rabern (1983), Chakrabarti (1983), Bjorhovde and Chakrabarti (1985), Gross and Cheok (1988), and Girard et al. (1995) verified the 30° stress trajectories. However, the experimental observations of Yamamoto et al. (1985) and Cheng and Grondin (1999) showed that the stress dispersion angle increases with inelastic material behavior. Cheng and Grondin (1999) recommended a 45° dispersion angle.

Dowswell (2006) reviewed the literature on gusset stability prior to 2006, including research by Chakrabarti (1987), Brown (1988), Gross and Cheok (1988), Yam and Cheng (1993), Rabinovitch and Cheng (1993), Walbridge et al. (1998), Nast et al. (1999), and Sheng et al. (2002). For the current paper, the data from Dowswell (2006) was combined with newer data from the research of Hamedani et al. (2011), Mentes (2011), Higgins et al. (2013), Naghipour et al. (2013), and White et al. (2013). The research projects included single- and double-plane gusset plates as well as corner- and extended-corner gusset plates. This paper used the results of experimental testing and inelastic finite element models from 12 separate projects with a total of 162 specimens.

VARIABLE STRESS TRAJECTORIES

Using fracture mechanics, Dowswell (2013) showed that the dispersion angle, θ, is dependent on geometry, constraint, and inelastic deformation capacity. The model in Figure 4(a), based on the stress-free zone ahead of a crack, was used to develop Equation 1, which accounts for all variables affecting the dispersion angle. Equation 1 is plotted in Figure 4(b).

$$\tan\theta = \frac{4C(\alpha - ½)}{\pi\lambda\beta^2} \tag{1}$$

where

C = constraint factor
= 1.00 for uniaxial stress
= 1.32 for constraint in one direction
= 2.27 for constraint in two directions

α = factor accounting for inelastic potential
= 1.0 for gusset plates with no inelastic capacity
= 1.7 for gusset plates with full inelastic potential

β = geometry factor

λ = inelastic material parameter calculated with Equation 2

$$\lambda = 1 + 0.77(\alpha - 1) \tag{2}$$

To determine θ as a function of α, substitute β = 1.0 for corner gusset plates, C = 1.0 for plates with uniaxial stress, and λ from Equation 2 into Equation 1 to get Equation 3.

$$\tan\theta = \frac{\alpha - ½}{0.605\alpha + 0.181} \tag{3}$$

Equation 3 results in trajectory angles of 32.5° for plates with no inelastic capacity and 44.8° for plates with full inelastic potential. The effective width, shown in Figure 5(a), is

$$b_e = 2a = 2l\tan\theta \tag{4}$$

where

a = crack half-length, in.

l = length, parallel to the load, of the connection between outermost fasteners, in.

In some cases, the effective width can extend beyond the free boundaries of the plate as shown in Figure 5(b), causing a smaller effective width than calculated with Equation 4.

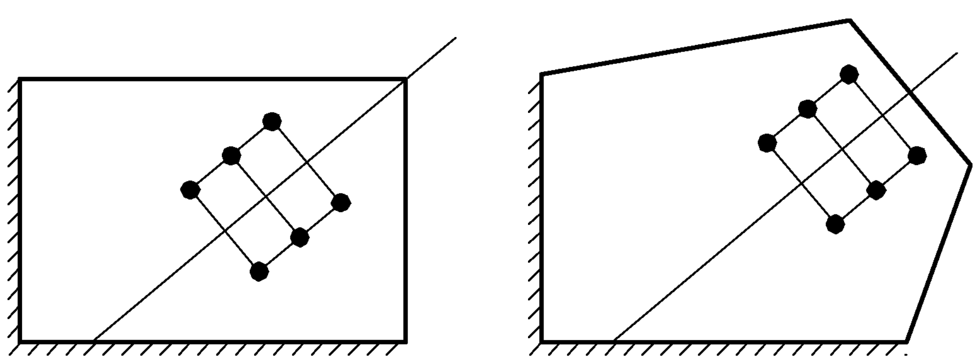

(a) corner gusset plate (b) extended corner gusset plate

Fig. 3. Gusset plate configurations.

The shaded portion of the stress trajectory is not effective, and the effective width is based on the actual plate width at the critical section. This effect was accounted for in the calculation of predicted strengths for validating the design procedure. For conditions where the effective width extended beyond the connected boundaries of the plate, the full effective width was used in the calculation of the predicted strength.

The trajectory angle for gusset plates subjected to tension is limited only by the rupture ductility, resulting in $\alpha = 1.7$ and $\theta = 45°$. For gusset plates in compression, α is dependent on the plate slenderness. Because the lateral buckling strength of the equivalent column is based on the AISC column curve, α can be calculated using AISC *Specification* Section E3. The column curve is in the inelastic range when $\lambda_c \le \lambda_r$, where $\lambda_r = 1.5$, and the slenderness parameter, λ_c, is calculated with Equation 5.

$$\lambda_c = \frac{KL}{\pi r}\sqrt{\frac{F_y}{E}} \tag{5}$$

where

E = modulus of elasticity, ksi
F_y = specified minimum yield strength, ksi
K = effective length factor
L = column length, in.
r = radius of gyration, in.
λ_c = slenderness parameter

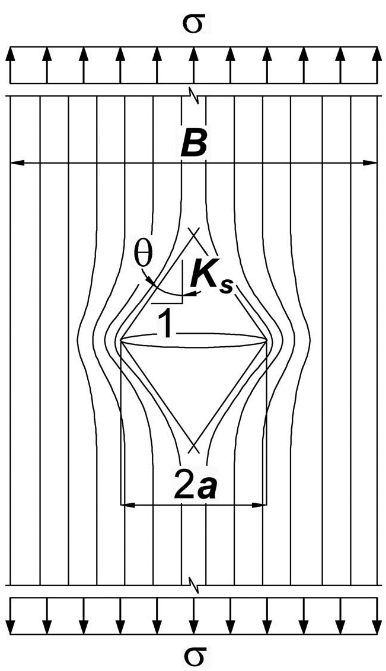

(a) stress-free zone ahead of a crack

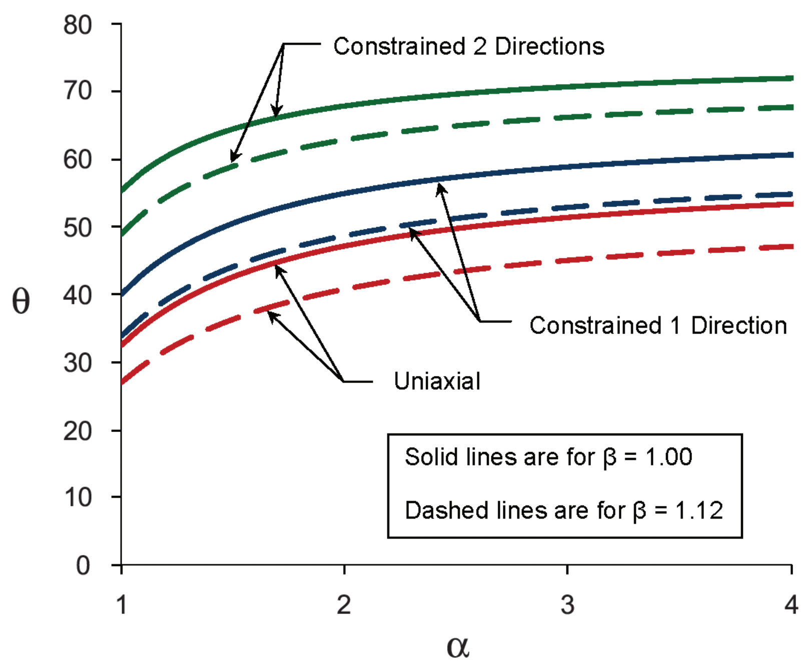

(b) dispersion angle vs. normalized strain

Fig. 4. Variable stress trajectories.

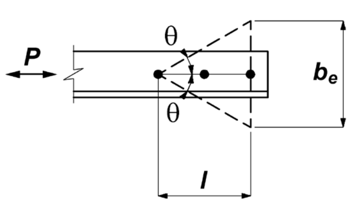

(a) variable effective width

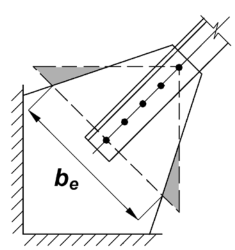

(b) maximum effective width

Fig. 5. Effective width.

λ_r = limiting slenderness parameter between elastic and inelastic behavior

For design purposes, linear interpolation can be used between $\alpha = 1.0$ and 1.7, resulting in Equation 6.

$$\alpha = 1.7 - 0.7\frac{\lambda_c}{\lambda_r} \geq 1.0 \tag{6}$$

Equation 6 is substituted into Equation 3 with $\lambda_r = 1.5$, resulting in Equation 7.

$$\tan\theta = \frac{1 - 0.389\lambda_c}{1 - 0.236\lambda_c} \tag{7}$$

Setting a lower limit of $\theta = 32.5°$, θ can be calculated with Equation 8, which results in $32.5° \leq \theta \leq 43.7°$.

$$\tan\theta = 0.956 – 0.213\lambda_c \geq 0.637 \tag{8}$$

Equation 5 is substituted into Equation 8, resulting in Equation 9.

$$\tan\theta = 0.956 - \frac{0.213K_\theta L}{\pi r}\sqrt{\frac{F_y}{E}} \geq 0.637 \tag{9}$$

To allow the use of different effective length factors in the stress dispersion angle and buckling strength calculations, K_θ was substituted for K in Equation 9.

EFFECTIVE LENGTH FACTORS

The dispersion angle, θ, defines the stress trajectory within the length of the fastener group; however, the stress continues to disperse through the gusset plate beyond the effective width as shown in Figure 6(a). This has a load-shedding effect on the equivalent column, where the load from the area bound by the effective width disperses into adjacent parts of the plate. The problem is similar to a column with a concentrated load at the top and a distributed load along the column length as shown in Figure 6(b). For corner gusset plates, the brace load also enters the framing members at the connected gusset boundaries, resulting in the shedding of a large portion of the load along the equivalent column length.

Another beneficial effect is the restraint from the relatively low-stress areas of the gusset plate adjacent to the equivalent column. Due to these and other effects discussed by Dowswell (2006), effective length factors for gusset plates cannot be estimated based on the buckled shape as they are for simple prismatic columns.

Effective length factors, both the effective width, K_θ, and buckling strength, K, calculations, were selected empirically, using the experiments and finite element models discussed in the Existing Research section of this paper. Although many of the specimens buckled in a sidesway mode, the empirical evidence shows that effective length factors much lower than the theoretical value of 1.0 can be safely used.

The effective length factors must be selected for use with a specific buckling length. Thornton (1984) originally proposed an effective length factor of 0.65 for use with a 30° stress dispersion angle and a buckling length, l_{avg}, which is the average of l_1, l_2, and l_3 as shown in Figure 2(b). When variable stress trajectories are used, the empirical data shows that a more accurate solution is obtained using a buckling length, $L = l_1$, which is the unsupported length along the center of the brace. Therefore, all effective length factors proposed in this paper have been calibrated for use with the unsupported length along the center of the brace.

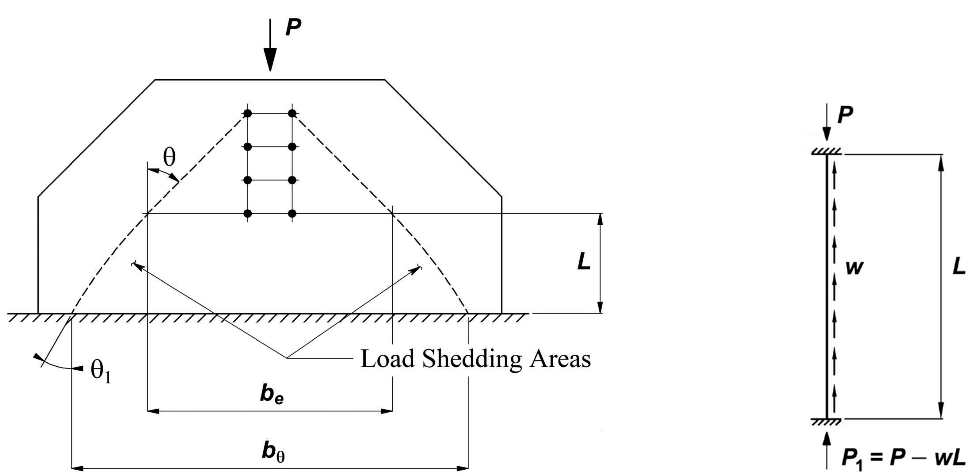

(a) gusset plate *(b) column model*

Fig. 6. Stress dispersion beyond the effective width.

RELIABILITY ANALYSIS

A reliability analysis was used to determine the most efficient combination of K_θ, K, and ϕ that provides a minimum β_R of 4.0, which is the applicable target reliability index for connections according to AISC *Specification* Section B3.1. Commentary. The buckling strength for the analysis was calculated using the provisions in AISC *Specification* Section J4.4 with the measured material and geometric properties of the experimental specimens. The reduction factor required to obtain a specific reliability level is (Galambos and Ravinda, 1978):

$$\phi = C_R \rho_R e^{-\beta_R \alpha_R V_R} \tag{10}$$

where

C_R = correction factor

V_R = coefficient of variation

α_R = separation factor

β_R = reliability index

ρ_R = bias coefficient

Galambos and Ravinda (1973) proposed a separation factor, α_R, of 0.55. For $L/D = 3.0$, Grondin et al. (2007) developed Equation 11 for calculating a correction factor, C, which is 0.900 at $\beta = 4.0$.

$$C_R = 1.4056 - 0.1584\,\beta_R + 0.008\,\beta_R^2 \tag{11}$$

The bias coefficient is

$$\rho_R = \rho_M\,\rho_G\,\rho_P \tag{12}$$

where

ρ_G = bias coefficient for the geometric properties

ρ_M = bias coefficient for the material properties

ρ_P = bias coefficient for the test-to-predicted strength ratios. Mean value of the professional factor is calculated with the measured geometric and material properties.

The coefficient of variation is

$$V_r = \sqrt{V_M^2 + V_G^2 + V_P^2} \tag{13}$$

where

V_G = coefficient of variation for the geometric properties

V_M = coefficient of variation for the material properties

V_P = coefficient of variation for the test-to-predicted strength ratios

Hess et al. (2002) recommended $\rho_G = 1.05$ and $V_G = 0.044$ for plate thickness variations. For the plate yield strength, $\rho_M = 1.11$ and $V_M = 0.054$ (Schmidt and Bartlett, 2002).

For corner gusset plates, the reliability analysis resulted in $K_\theta = 0.85$, $K = 0.40$, and $\phi = 0.75$ at $\beta_R = 4.0$. With these values, the mean ratio of the professional factor, ρ_P, is 1.12 and the coefficient of variation, V_P, is 0.192. Dowswell (2018), who analyzed the reliability of several existing design methods, showed that the minimum V_p for all of the existing methods is 0.270. Therefore, the proposed design method is substantially more accurate than the existing methods.

Because only 13 specimens are available for extended corner gusset plates, a reliability analysis was not conducted. With $K_\theta = 0.85$ and $K = 0.50$, $\rho_P = 1.15$, $V_P = 0.129$, and the minimum professional factor is 0.840. Although a lower value could potentially be justified, it is believed that, until further research is available, $K = 0.50$ provides a reasonable fit for extended corner gusset plates.

DESIGN MODEL

For the proposed design model, $K_\theta = 0.85$ and $r = t/\sqrt{12}$ were substituted into Equation 9 and the equation was adjusted so the trajectory angles are within $30° \le \theta \le 45°$, resulting in Equation 14.

$$\tan\theta = 1 - \frac{L}{5t}\sqrt{\frac{F_y}{E}} \ge \tan 30° \tag{14}$$

The effective width, b_e, is calculated with Equation 4; however, b_e is limited to the actual plate width at the critical section as shown in Figure 5(b). The equivalent rectangular column, $b_e \times t$, is designed according to AISC *Specification* Section J4.4 using $\phi = 0.75$ in lieu of 0.90. The length of the equivalent column, L, is defined along the center of the brace as shown in Figure 7, with $K = 0.40$ for corner gusset plates and $K = 0.50$ for extended corner gusset plates.

Results of experimental testing and finite element models discussed in the Existing Research section of this paper are compared to the predicted strengths from the design model in Tables A1 and A2 of Appendix A. The normalized experimental load, P_e/P_y, is plotted against λ_c in Figure 8. P_e is the experimental strength and $P_y = \sigma_y b_e t$ is the axial yield load of the equivalent column, based on the measured yield stress, σ_y.

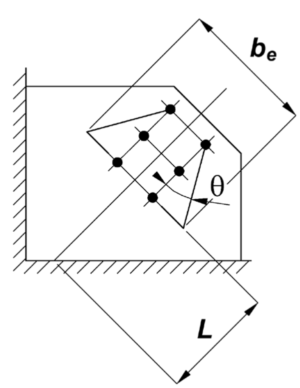

Fig. 7. Gusset geometry for proposed design procedure.

CONCLUSIONS

Gusset plates subjected to compression loads are currently designed with an equivalent column model, where the width of the equivalent column is defined by a 30° stress dispersion angle. However, both experimental and theoretical research has shown that the dispersion angle is partially dependent on the inelastic deformation capacity of the plate. To account for this behavior, a new design model for buckling of corner gusset plates has been developed. The model is valid for single- and double-plane corner gusset plates, including extended corner gusset plates commonly used for seismic design.

The design model, based on the equivalent column concept, allows variable trajectories which are dependent on the level of inelasticity that can be reached prior to buckling. A reliability analysis using the results of 162 specimens from 14 previously-published research projects showed that the buckling strength can be calculated using the provisions in AISC *Specification* Section J4.4 with $\phi = 0.75$ in lieu of 0.90. The length of the equivalent column, L, is defined along the center of the brace with $K = 0.40$ for corner gusset plates and $K = 0.50$ for extended corner gusset plates. The proposed design model was shown to produce more accurate results than the existing design methods.

DESIGN EXAMPLE

Given:

Determine the buckling strength of the gusset plate in Figure 9. The gusset plate is ½-in. thick ASTM A572 Grade 50 material, and the factored brace axial compression load is 800 kips.

Solution:

From AISC *Manual* Table 2-4
ASTM A572, Grade 50
$F_y = 50$ ksi

From AISC *Manual* Table 1-1
W14×109
$d = 14.3$ in.

W21×132
$d = 21.8$ in.

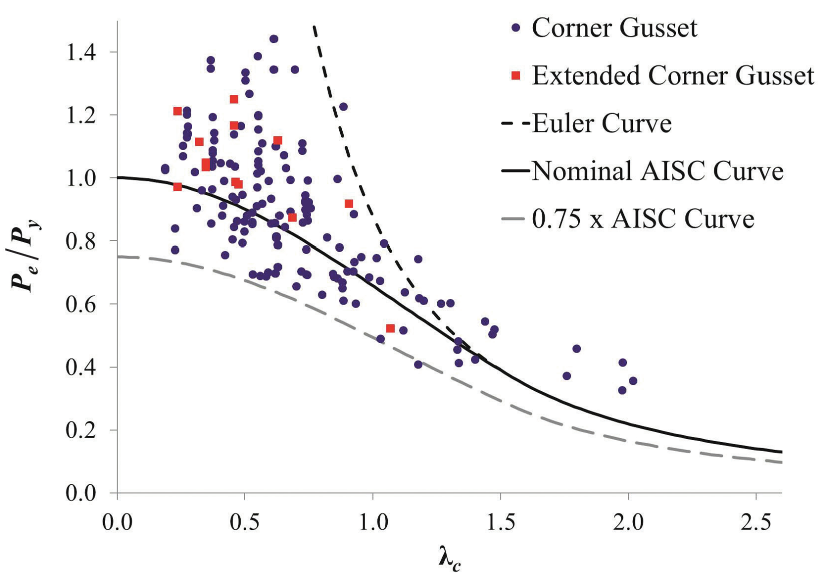

Fig. 8. Normalized load vs. slenderness for proposed design procedure.

$$L = 34\text{ in.} - \frac{21.8\text{ in.}}{2\cos 50°}$$
$$= 17.0\text{ in.}$$

$$\tan\theta = 1 - \frac{L}{5t}\sqrt{\frac{F_y}{E}} \geq \tan 30° \tag{14}$$
$$= 1 - \frac{17.0\text{ in.}}{(5)(0.500\text{ in.})}\sqrt{\frac{50\text{ ksi}}{29{,}000\text{ ksi}}} \geq \tan 30°$$
$$\theta = 35.7°$$

The gage in the 4-in. leg of the L6×4×¾, g, is 2.50 in.

The distance between bolts perpendicular to the load, w, is:

$$w = d + 2g$$
$$= 14.3\text{ in.} + 2(2.5\text{ in.})$$
$$= 19.3\text{ in.}$$

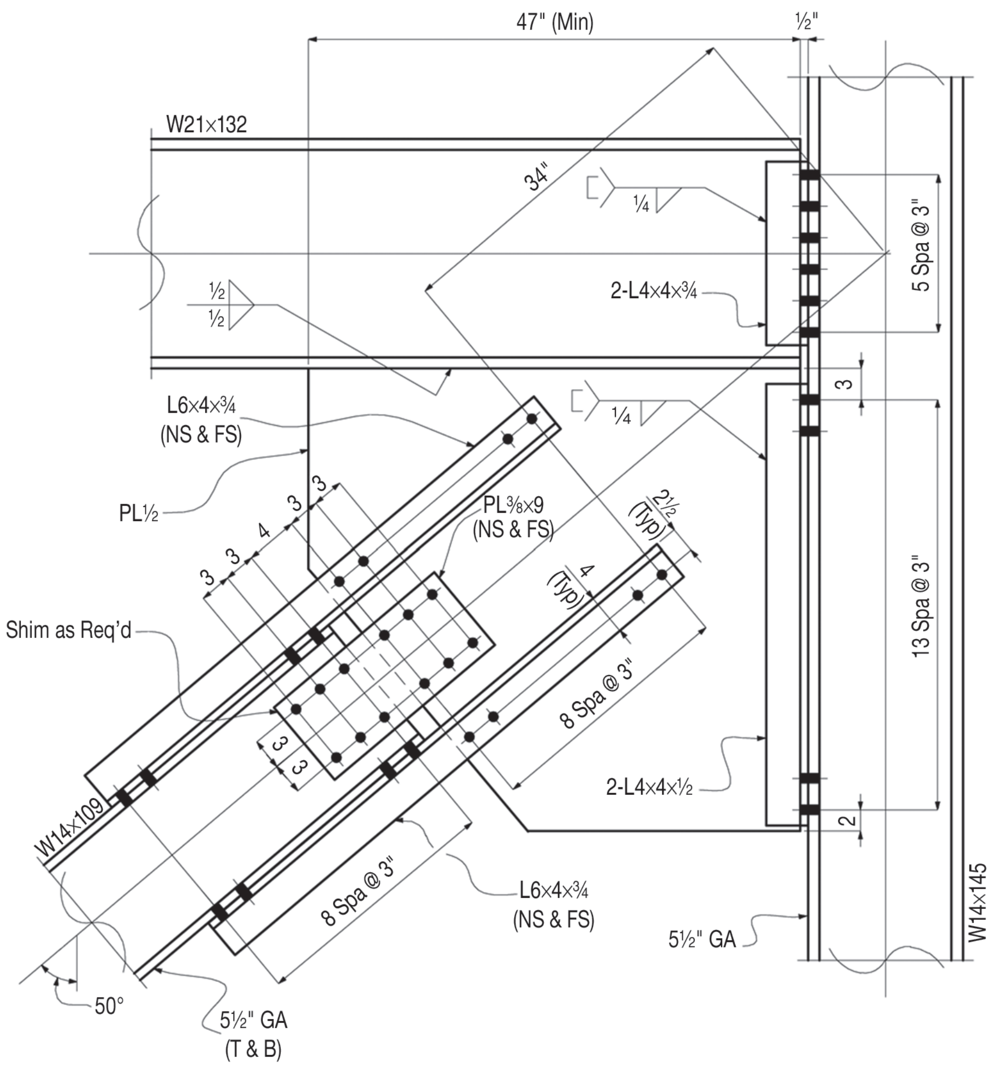

Fig. 9. Vertical bracing connection for Design Example.

The distance between bolts, parallel to the load, l, is:

$$\begin{aligned} l &= 8(3 \text{ in.}) \\ &= 24.0 \text{ in.} \end{aligned}$$

$$\begin{aligned} b_e &= 2l \tan\theta + w \\ &= \left[2(24 \text{ in.})\tan(35.7°)\right] + 19.3 \text{ in.} \\ &= 53.8 \text{ in.} \end{aligned}$$

$$\begin{aligned} A_g &= (0.500 \text{ in.})(53.8 \text{ in.}) \\ &= 26.9 \text{ in.}^2 \end{aligned}$$

$$\begin{aligned} r &= \frac{t}{\sqrt{12}} \\ &= \frac{0.500 \text{ in.}}{\sqrt{12}} \\ &= 0.144 \text{ in.} \end{aligned}$$

Because the line through the innermost bolts, perpendicular to the brace line of action, intersects both the beam and column interfaces, the plate is classified as a corner gusset; therefore, $K = 0.40$.

$$\begin{aligned} L_c &= KL \\ &= (0.4)(17.0 \text{ in.}) \\ &= 6.80 \text{ in.} \end{aligned}$$

$$\begin{aligned} \frac{L_c}{r} &= \frac{6.80 \text{ in.}}{0.144 \text{ in.}} \\ &= 47.2 \end{aligned}$$

Because $\frac{L_c}{r} = 47.2 > 25$, AISC *Specification* Section J4.4 specifies that the compression strength is calculated according to AISC *Specification* Section E3.

The elastic buckling stress, F_e, is calculated using AISC *Specification* Equation E3-4:

$$\begin{aligned} F_e &= \frac{\pi^2 E}{\left(\frac{L_c}{r}\right)^2} \qquad \text{(}\textit{Spec}\text{. Eq. E3-4)} \\ &= \frac{\pi^2(29{,}000 \text{ ksi})}{(47.2)^2} \\ &= 128 \text{ ksi} \end{aligned}$$

$$\begin{aligned} 4.71\sqrt{\frac{E}{F_y}} &= 4.71\sqrt{\frac{29{,}000 \text{ ksi}}{50 \text{ ksi}}} \\ &= 113 \end{aligned}$$

Because $\frac{L_c}{r} = 47.2 < 113$, the critical stress, F_{cr}, is calculated using AISC *Specification* Equation E3-2.

$$F_{cr} = \left(0.658^{\frac{F_y}{F_e}}\right)F_y \quad \text{(}Spec\text{. Eq. E3-2)}$$

$$= \left(0.658^{\frac{50\text{ ksi}}{128\text{ ksi}}}\right)(50\text{ ksi})$$

$$= 42.5\text{ ksi}$$

And the nominal compressive strength, P_n, is calculated using AISC *Specification* Equation E3-1.

$$P_n = F_{cr}A_g \quad \text{(}Spec\text{. Eq. E3-1)}$$

$$= (42.5\text{ ksi})(26.9\text{ in.}^2)$$

$$= 1{,}140\text{ kips}$$

The available compression strength is then:

$$\phi P_n = (0.75)(1{,}140\text{ kips})$$

$$= 855\text{ kips} > 800\text{ kips} \quad \textbf{o.k.}$$

For the Dowswell (2006) method, the gusset is compact; therefore, the compression strength is based on Whitmore yielding. $P_n =$ 1,180 kips, which is 3.51% higher than the strength calculated with the proposed method.

For the Thornton (1984) method, $L = l_{avg} = 4.71$ in. and $K = 0.65$. Because $KL/r < 25$, the compression strength is based on Whitmore yielding. $P_n = 1{,}180$ kips, which is 3.51% higher than the strength calculated with the proposed method.

For this example, the nominal strength calculated with the proposed method is similar to the nominal strengths calculated with both the Thornton (1984) and Dowswell (2006) methods. However, the reliability analysis showed that the proposed method is significantly more accurate than the existing methods for a wide range of slenderness values, potentially resulting in increased available strengths, ϕP_n, if all methods use a target reliability index of 4.0. Also, the proposed method more accurately models the stress trajectories in the gusset plate.

APPENDIX A TABLES

Table A1. Details of Corner Gusset Plates

Specimen	t in.	F_y ksi	E ksi	L in.	θ deg	b_e in.	P_c kips	P_e kips	P_e/P_c
Chakrabarti (1987)									
1	0.250	36.0	29000	8.00	37.8	9.20	74.6	68.7	0.920
2	0.250	36.0	29000	8.50	37.3	9.08	72.7	70.3	0.966
3	0.250	36.0	29000	8.00	37.8	9.20	74.6	71.4	0.957
Brown (1988)									
1-4-45-8	0.251	48.0	29500	7.75	36.9	10.8	114	180	1.58
2-3-45-4	0.196	45.2	29500	5.18	38.4	11.9	96.6	120	1.24
3-3-45-8	0.198	45.2	29500	7.75	34.7	10.2	75.7	82.0	1.08
9-3-55-4	0.192	45.2	29500	4.68	39.0	12.1	97.8	79.6	0.814
10-3-45-4	0.197	45.2	29500	5.26	38.3	11.9	96.6	110	1.13
11-4-40-8	0.250	48.0	29500	7.26	37.4	10.9	117	166	1.42
13-4-30-8	0.248	48.0	29500	6.16	38.6	11.2	123	139	1.13
14-4-30-4	0.248	48.0	29500	3.16	41.9	13.5	157	135	0.859
15-4-35-8	0.250	48.0	29500	6.80	38.0	11.0	120	154	1.29
16-4-35-4	0.250	48.0	29500	4.65	40.4	12.7	146	147	1.01
17-3-45-8	0.194	45.2	29500	7.79	34.4	10.2	73.0	120	1.64
18-4-45-4	0.251	48.0	29500	5.71	39.2	12.2	138	155	1.12
20-6-30-4	0.376	45.0	28300	4.81	41.9	13.5	223	176	0.789
Gross and Cheok (1988)									
1A	0.250	46.7	29000	8.01	36.6	8.94	91.3	116	1.27
1B	0.250	46.7	29000	8.01	36.6	8.94	91.3	96.0	1.05
2A	0.250	46.7	29000	8.63	35.9	8.78	87.7	138	1.57
2B	0.250	46.7	29000	8.63	35.9	8.78	87.7	148	1.69
3B	0.250	46.7	29000	8.51	36.0	8.82	88.4	88.0	1.00
Rabinovitch and Cheng (1993)									
A1	0.367	65.1	29878	8.72	37.9	19.9	430	378	0.879
A2	0.243	64.3	29878	8.72	33.7	17.5	218	254	1.16
A3	0.367	65.1	29878	8.72	37.9	19.9	430	451	1.05
A4	0.243	64.3	29878	8.72	33.7	17.5	218	258	1.18
Yam and Cheng (1993)									
GP1	0.524	42.8	30110	8.56	41.2	17.2	373	440	1.18
GP2	0.386	44.2	30487	8.56	39.7	16.4	264	305	1.15
GP3	0.256	39.9	28428	8.56	36.9	15.1	135	167	1.23
GP1R	0.524	42.8	30110	8.56	41.2	17.2	373	462	1.24
GP2R	0.386	44.2	30487	8.56	39.7	16.4	264	334	1.26
GP3R	0.256	39.9	28428	8.56	36.9	15.1	135	178	1.31
AP1	0.524	42.8	30110	9.58	40.8	16.9	365	387	1.06
AP2	0.386	44.2	30487	9.58	39.0	16.1	255	272	1.07
AP3	0.256	39.9	28428	9.58	35.7	14.6	127	164	1.29
MP1	0.524	42.8	30110	8.56	41.2	17.2	373	435	1.17
MP2	0.386	44.2	30487	8.56	39.7	16.4	264	296	1.12
MP3	0.256	39.9	28428	8.56	36.9	15.1	135	162	1.20
MP3A	0.256	39.9	28428	8.56	36.9	15.1	135	184	1.36
MP3B	0.256	39.9	28428	8.56	36.9	15.1	135	185	1.36
SP1-Free	0.524	42.8	30110	19.7	35.6	22.4	426	361	0.848
SP2-Free	0.386	44.2	30487	19.7	31.4	19.5	244	227	0.930
SP1-Fixed	0.524	42.8	30110	19.7	35.6	22.4	426	396	0.929
SP2-Fixed	0.386	44.2	30487	19.7	31.4	19.5	244	332	1.36

Table A1. Details of Corner Gusset Plates (continued)									
Specimen	t in.	F_y ksi	E ksi	L in.	θ deg	b_e in.	P_c kips	P_e kips	P_e/P_c
Walbridge et al. (1998)									
GP1B1	0.236	43.5	29878	8.72	35.7	18.6	163	155	0.952
GP1B3	0.236	43.5	29878	8.72	35.7	18.6	163	156	0.957
GP2B7	0.354	43.5	29878	8.72	39.1	20.7	296	290	0.980
GP3B11	0.472	43.5	29878	8.72	40.7	21.7	428	403	0.941
GP1MC20	0.524	42.8	30110	8.56	41.2	17.1	372	466	1.25
GP2MC22	0.386	44.2	30487	8.56	39.7	16.4	264	302	1.14
GP3MC24	0.256	39.9	28428	8.56	36.9	15.0	135	160	1.18
A2CL2	0.243	64.3	29878	8.72	33.7	17.5	218	246	1.13
A4CL4	0.243	64.3	29878	8.72	33.7	17.5	218	252	1.15
Nast et al. (1999)									
T2-FE	0.378	61.5	31256	8.72	38.5	20.3	434	444	1.02
T2	0.378	61.5	31256	8.72	38.5	20.3	434	380	0.876
Sheng et al. (2002)									
500×400×13.3×240	0.524	42.8	29008	11.3	39.8	11.9	251	366	1.45
500×400×13.3×310	0.524	42.8	29008	8.56	41.2	17.1	372	447	1.20
500×400×13.3×380	0.524	42.8	29008	5.80	42.5	22.8	504	528	1.05
750×400×13.3×240	0.524	42.8	29008	11.3	39.8	11.9	251	359	1.43
750×400×13.3×310	0.524	42.8	29008	8.56	41.2	17.1	372	438	1.18
750×400×13.3×380	0.524	42.8	29008	5.80	42.5	22.8	504	525	1.04
500×400×9.87×240	0.389	44.2	29008	11.3	37.7	11.2	173	257	1.48
500×400×9.87×310	0.389	44.2	29008	8.56	39.6	16.4	265	322	1.22
500×400×9.87×380	0.389	44.2	29008	5.80	41.5	22.2	370	420	1.13
750×400×9.87×240	0.389	44.2	29008	11.3	37.7	11.2	173	252	1.46
750×400×9.87×310	0.389	44.2	29008	8.56	39.6	16.4	265	315	1.19
750×400×9.87×380	0.389	44.2	29008	5.80	41.5	22.2	371	408	1.10
500×400×6.5×240	0.256	39.9	29008	11.3	33.9	10.1	82.7	114	1.38
500×400×6.5×310	0.256	39.9	29008	8.56	37.0	15.1	136	156	1.15
500×400×6.5×380	0.256	39.9	29008	5.80	39.8	21.0	203	222	1.10
750×400×6.5×240	0.256	39.9	29008	11.3	33.9	10.1	82.7	112	1.35
750×400×6.53×10	0.256	39.9	29008	8.56	37.0	15.1	136	150	1.10
750×400×6.5×380	0.256	39.9	29008	5.80	39.8	21.0	203	207	1.02
Hamedani et al. (2011)									
GP1	0.524	42.8	30110	8.56	41.2	17.2	373	462	1.24
GP2	0.386	44.2	30487	8.56	39.7	16.4	264	312	1.18
GP3	0.256	39.9	28428	8.56	36.9	15.1	135	172	1.27
Hafner (2012)									
1	0.250	47.0	29000	28.4	30.0	34.8	88.1	146	1.66
2	0.250	45.1	29000	28.4	30.0	34.8	88.1	163	1.85
3	0.375	45.9	29000	28.4	30.0	34.8	286	273	0.955
4	0.250	45.1	29000	28.4	30.0	34.8	88.1	128	1.45
5	0.375	46.1	29000	28.4	30.0	34.8	286	290	1.01
6	0.375	46.3	29000	28.4	30.0	34.8	286	249	0.869

Table A1. Details of Corner Gusset Plates (continued)									
Specimen	t in.	F_y ksi	E ksi	L in.	θ deg	b_e in.	P_c kips	P_e kips	P_e/P_c
Mentes (2011)									
GP307-SS3	0.375	36.4	29000	13.1	37.0	28.8	347	358	1.03
GP307-LS3	0.375	48.2	29000	18.1	31.2	28.2	372	398	1.07
GP490-SS3	0.375	46.4	29000	13.1	35.8	24.4	362	364	1.00
GP490-LS3-1	0.375	45.9	29000	18.1	31.6	22.3	285	264	0.928
Naghipour et al. (2013)									
1	0.157	53.7	30458	16.6	30.0	9.91	19.2	25.3	1.32
2	0.157	53.7	30458	13.9	30.0	13.1	36.4	45.2	1.24
3	0.157	53.7	30458	11.1	30.0	16.3	62.5	82.9	1.33
4	0.157	53.7	30458	8.3	30.9	20.1	99.2	169	1.70
5	0.315	53.7	30458	22.2	30.0	9.91	76.2	55.6	0.729
6	0.315	53.7	30458	19.4	30.0	13.1	115	88.0	0.764
7	0.315	53.7	30458	16.7	30.9	16.8	166	141	0.849
8	0.315	53.7	30458	13.9	33.7	21.9	239	232	0.971
9	0.315	53.7	30458	11.2	36.2	27.7	328	377	1.15
10	0.472	53.7	30458	21.4	33.3	10.8	175	201	1.15
11	0.472	53.7	30458	18.7	35.1	15.1	260	321	1.24
12	0.472	53.7	30458	15.9	36.7	20.0	360	420	1.17
13	0.472	53.7	30458	13.1	38.3	25.3	475	485	1.02
14	0.472	53.7	30458	10.4	39.8	31.1	605	547	0.905
15	0.630	53.7	30458	28.3	33.5	10.8	235	274	1.17
16	0.630	53.7	30458	25.5	34.8	15.0	340	409	1.20
17	0.630	53.7	30458	22.8	36.0	19.6	461	501	1.09
18	0.630	53.7	30458	20.0	37.2	24.5	597	597	1.00
19	0.630	53.7	30458	17.2	38.4	29.8	748	690	0.922
Test	0.315	53.7	30458	16.6	31.0	10.2	101	90.7	0.899
20	0.315	53.7	30458	16.6	31.0	10.2	101	93.4	0.926
White et al. (2013)									
P5U-WV-NP-01	0.250	53.0	29000	23.8	30.0	43.2	155	263	1.69
	0.313	53.0	29000	23.8	30.0	43.2	301	390	1.30
	0.375	53.0	29000	23.8	30.0	43.2	471	525	1.12
	0.400	53.0	29000	23.8	30.0	43.2	540	585	1.08
	0.438	53.0	29000	23.8	30.0	43.2	644	675	1.05
	0.500	53.0	29000	23.8	30.7	43.8	828	818	0.987
	0.625	53.0	29000	23.8	34.0	46.0	1227	1073	0.874
P6U-WV-NP-02	0.250	53.0	29000	18.5	30.0	46.2	270	260	0.963
	0.313	53.0	29000	18.5	30.0	46.2	453	396	0.873
	0.375	53.0	29000	18.5	30.0	46.2	638	554	0.868
	0.438	53.0	29000	18.5	32.5	49.4	878	723	0.824
	0.500	53.0	29000	18.5	34.3	51.9	1121	904	0.807
	0.600	53.0	29000	18.5	36.4	54.7	1510	1198	0.793
	0.625	53.0	29000	18.5	36.7	55.3	1607	1266	0.787
P8U-WV-INF-02	0.500	53.0	29000	25.3	30.0	49.6	900	987	1.10
P13U-W-NP-01	0.250	53.0	29000	19.6	30.0	46.6	249	322	1.30
	0.313	53.0	29000	19.6	30.0	46.6	431	479	1.11
	0.375	53.0	29000	19.6	30.0	46.6	618	636	1.03
	0.400	53.0	29000	19.6	30.2	46.9	697	702	1.01

Specimen	t in.	F_y ksi	E ksi	L in.	θ deg	b_e in.	P_c kips	P_e kips	P_e/P_c
Table A1. Details of Corner Gusset Plates (continued)									
White et al. (2013) continued									
	0.438	53.0	29000	19.6	31.7	49.1	845	792	0.937
	0.500	53.0	29000	19.6	33.7	51.9	1096	957	0.873
	0.625	53.0	29000	19.6	36.2	54.4	1557	1263	0.811
E1W-307SS	0.250	36.4	29000	13.1	32.2	25.7	177	190	1.07
	0.313	36.4	29000	13.1	35.1	27.6	262	265	1.01
	0.438	36.4	29000	13.1	38.2	29.7	432	409	0.947
	0.500	36.4	29000	13.1	39.2	30.4	515	487	0.945
E2W-307LS	0.250	48.2	29000	18.1	30.0	27.3	162	199	1.23
	0.313	48.2	29000	18.1	30.0	27.3	261	327	1.25
	0.438	48.2	29000	18.1	33.5	29.9	500	546	1.09
	0.500	48.2	29000	18.1	35.2	31.1	521	653	1.25
	0.625	48.2	29000	18.1	37.4	32.9	664	852	1.28
E3W-307SL	0.250	46.6	29000	13.1	30.1	33.2	270	284	1.05
	0.313	46.6	29000	13.1	33.6	36.6	423	369	0.872
	0.375	46.6	29000	13.1	35.8	38.8	578	473	0.818
	0.438	46.6	29000	13.1	37.2	40.4	733	573	0.782
E4W-490SS	0.250	46.4	29000	13.1	30.2	21.6	175	222	1.27
	0.313	46.4	29000	13.1	33.6	23.3	269	299	1.11
	0.438	46.4	29000	13.1	37.3	25.2	455	437	0.960
E5W-490LS	0.250	45.6	29000	18.1	30.0	21.5	126	148	1.18
	0.313	45.6	29000	18.1	30.0	21.5	200	230	1.15
	0.438	45.6	29000	18.1	33.9	23.4	376	402	1.07
	0.500	45.6	29000	18.1	35.5	24.3	468	488	1.04
	0.625	45.6	29000	18.1	37.6	25.4	650	638	0.981

Specimen	t in.	F_y ksi	E ksi	L in.	θ deg	b_e in.	P_c kips	P_e kips	P_e/P_c
Table A2. Details of Extended Corner Gusset Plates									
Sheng et al. (2002)									
440×310×13.3×240	0.524	42.8	29008	11.3	39.8	11.9	244	333	1.36
440×310×13.3×310	0.524	42.8	29008	8.56	41.2	17.1	365	403	1.10
440×310×13.3×380	0.524	42.8	29008	5.80	42.5	22.8	499	496	0.994
390×200×13.3×240	0.524	42.8	29008	11.3	39.8	10.6	217	277	1.27
390×200×13.3×310	0.524	42.8	29008	8.56	41.2	14.4	308	335	1.09
390×200×13.3×380	0.524	42.8	29008	5.80	42.5	17.0	373	463	1.24
390×200×9.87×240	0.389	44.2	29008	11.3	37.7	10.2	149	197	1.32
390×200×9.87×310	0.389	44.2	29008	8.56	39.6	14.4	226	243	1.08
390×200×9.87×380	0.389	44.2	29008	5.80	41.5	17.0	281	327	1.16
390×200×6.5×240	0.256	39.9	29008	11.3	33.9	9.69	70.3	90.8	1.29
390×200×6.5×310	0.256	39.9	29008	8.56	37.0	14.1	118	126	1.06
390×200×6.5×380	0.256	39.9	29008	5.80	39.8	17.0	159	172	1.08
Rabinovitch and Cheng (1993)									
A5	0.367	65.1	29878	15.2	31.6	16.3	242	204	0.843

SYMBOLS

C Constraint factor

C_R Correction factor

E Modulus of elasticity, ksi

F_y Specified minimum yield strength, ksi

K Effective length factor used in the buckling strength calculation

K_θ Effective length factor used for calculating the stress dispersion angle, θ

L Column length, in.

V_G Coefficient of variation for the geometric properties

V_M Coefficient of variation for the material properties

V_P Coefficient of variation for the test-to-predicted strength ratios

V_R Coefficient of variation

a Crack half-length, in.

b_e Effective width, in.

l Length, parallel to the load, of the connection between outermost fasteners, in.

r Radius of gyration, in.

α Factor accounting for inelastic potential

α_R Separation factor

β Geometry factor

β_R Reliability index

λ Inelastic material parameter

λ_c Slenderness parameter

λ_r Limiting slenderness parameter between elastic and inelastic behavior

ϕ Reduction factor for designing according to LRFD

ρ_G Bias coefficient for the geometric properties

ρ_M Bias coefficient for the material properties

ρ_P Bias coefficient for the test-to-predicted strength ratios. Mean value of the professional factor calculated with the measured geometric and material properties.

ρ_R Bias coefficient

θ Stress dispersion angle, deg

REFERENCES

AISC (2016), *Specification for Structural Steel Buildings*, ANSI/AISC 360–16, American Institute of Steel Construction, Chicago, Ill.

Bjorhovde, R. and Chakrabarti, S.K. (1985), “Tests of Full-size Gusset Plate Connections,” *Journal of Structural Engineering,* ASCE, Vol. 111, No. 3, March, pp. 667–683.

Brown, V.L. (1988), *Stability of Gusseted Connections in Steel Structures*, Doctoral Dissertation, University of Delaware, Newark, Del.

Chakrabarti, S.K. (1983), *Tests of Gusset Plate Connections,* M.S. Thesis, University of Arizona, Tucson, Ariz.

Chakrabarti, S.K. (1987), *Inelastic Buckling of Gusset Plates*, Doctoral Dissertation, University of Arizona, Tucson, Ariz.

Cheng, J.J.R. and Grondin, G.Y. (1999), “Recent Developments in the Behavior of Cyclically Loaded Gusset Plate Connections,” *Proceedings of the North American Steel Construction Conference*, AISC, Las Vegas, Nev., pp. 8–1 through 8–22.

Dowswell, B. (2006), “Effective Length Factors for Gusset Plate Buckling,” *Engineering Journal*, AISC, Vol. 43, No. 2.

Dowswell, B. (2013), “Calculation of Stress Trajectories Using Fracture Mechanics,” *Engineering Journal*, AISC, Vol. 50, No. 1.

Dowswell, B. (2016), “Stability of Rectangular Connection Elements,” *Engineering Journal*, AISC, Vol. 53, No. 4.

Dowswell, B. (2018), “Reliability of the Equivalent Column Method for Corner Gusset Plates,” *Engineering Journal*, AISC, Submitted for Review.

Galambos, T.V. and Ravinda, M.K. (1973), “Tentative Load and Resistance Factor Design Criteria for Steel Buildings,” Research Report No. 18, Department of Civil and Environmental Engineering, September, Washington University, St. Louis, Mo.

Galambos, T.V. and Ravinda, M.K. (1978), “Properties of Steel for Use in LRFD,” *Journal of the Structural Division*, ASCE, Vol. 104, No. ST9, September, pp. 1,459–1,468.

Girard, C., Picard, A., and Fafard, M. (1995), “Finite Element Modeling of the Shear Lag Effects in an HSS Welded to a Gusset Plate,” *Canadian Journal of Civil Engineering*, Vol. 22, pp. 651–659.

Grondin, G., Jin, M., and Josi, G. (2007), “Slip Critical Bolted Connections—A Reliability Analysis for Design at the Ultimate Limit State,” Structural Engineering Report No. 274, Department of Civil Engineering, October, University of Alberta, Alberta, Canada.

Gross, J.L. and Cheok, G. (1988), *Experimental Study of Gusseted Connections for Laterally Braced Steel Buildings*, National Institute of Standards and Technology, Gaithersburg, Md.

Hamedani, H., Gholampour, S., and Yadollahi, Y. (2011), "The Effect of Edge Stiffener on Compressive Behavior of Gusset Plate," *Proceedings of the Fifth Symposium on Advances in Science and Technology*, Mashhad, Iran.

Hafner, A.G. (2012), *Experimental Research on the Behavior and Strength of Large-Scale Steel Gusset Plates with Sway-buckling Response Including Effects of Corrosion and Retrofit Options*, Master's Thesis, Oregon State University, Corvallis, Ore., March 20.

Hess, P.E., Bruchman, D., Assakkaf, I.A., and Ayyub, B.M. (2002), "Uncertainties in Material Strength, Geometric and Load Variables," *Naval Engineers Journal*, Vol. 114, No. 2, April, pp. 139–166.

Higgins, C., Hafner, A., Turan, O., and Schumacher, T. (2013). "Experimental Tests of Truss Bridge Gusset Plate Connections with Sway-Buckling Response," *Journal of Bridge Engineering*, Vol. 18, No. 10, pp. 980–991.

Lavis, C.S. (1967), *Computer Analysis of the Stresses in a Gusset Plate*, Master's Thesis, University of Washington, Seattle, Wash.

Mentes, Y. (2011), *Analytical and Experimental Assessment of Steel Truss Bridge Gusset Plate Connections*, Doctoral Dissertation, Georgia Institute of Technology, Atlanta, Ga.

Muir, L.S. and Thornton, W.A. (2014), *Vertical Bracing Connections—Analysis and Design*, Design Guide 29, AISC, Chicago, Ill.

Naghipour, M., Abdollahzadeh, G., and Shokri, M. (2013), "Analysis and Design Procedure of Corner Gusset Plate Connections in BRBFs," *Iranica Journal of Energy and Environment*, Vol. 4, pp. 271–282.

Nast, T.E., Grondin, G.Y., and Cheng, J.J.R. (1999), *Cyclic Behavior of Stiffened Gusset Plate Brace Member Assemblies*, University of Alberta Department of Civil and Environmental Engineering Structural Engineering Report No. 229, University of Alberta, Alberta, Canada.

Rabern, D.A. (1983), *Stress, Strain and Force Distributions in Gusset Plate Connections*, Master's Thesis, University of Arizona, Tucson, Ariz.

Rabinovitch, J. and Cheng, J.J.R. (1993), *Cyclic Behavior of Steel Gusset Plate Connections*, University of Alberta Department of Civil Engineering Structural Engineering Report No. 191, University of Alberta, Alberta, Canada.

Sandel, J.A. (1950), *Photoelastic Analysis of Gusset Plates*, Master's Thesis, University of Tennessee, Knoxville, Tenn.

Schmidt, B.J. and Bartlett, F.M. (2002), "Review of Resistance Factor for Steel: Data Collection," *Canadian Journal of Civil Engineering*, Vol. 29, pp. 98–108.

Sheng, N., Yam, C.H., and Iu, V.P. (2002), "Analytical Investigation and the Design of the Compressive Strength of Steel Gusset Plate Connections," *Journal of Constructional Steel Research*, Vol. 58, pp. 1,473–1,493.

Thornton, W.A. (1984), "Bracing Connections for Heavy Construction," *Engineering Journal*, AISC, Vol. 21, No. 3, pp. 139–148.

Walbridge, S.S., Grondin, G.Y., and Cheng, J.J.R. (1998), *An Analysis of the Cyclic Behavior of Steel Gusset Plate Connections*, University of Alberta Department of Civil and Environmental Engineering Structural Engineering Report No. 225, University of Alberta, Alberta, Canada.

Whitmore, R.E. (1952), *Experimental Investigation of Stresses in Gusset Plates*, University of Tennessee Engineering Experiment Station Bulletin No. 16, University of Tennessee, Knoxville, Tenn.

White, D.W., Leon, R.T., Kim, Y.D., Mentes, Y., and Bhuiyan, M.T.R. (2013), *Finite Element Simulation and Assessment of the Strength Behavior of Riveted and Bolted Gusset-Plate Connections in Steel Truss Bridges*, Final Report Prepared for Federal Highway Administration and NCHRP Transportation Research Board, March.

Wyss, T. (1923), "Die Kraftfelder in Festen Elastischen Korpern und ihre Praktischen Anwendungen," Berlin.

Yamamoto, K., Akiyama, N., and Okumara, T. (1985), "Elastic Analysis of Gusseted Truss Joints," *Journal of Structural Engineering,* ASCE, Vol. 111, No. 12, December, pp. 2,545–2,564.

Yam, M.C.H. and Cheng, J.J.R. (1993), *Experimental Investigation of the Compressive Behavior of Gusset Plate Connections*, University of Alberta Department of Civil Engineering Structural Engineering Report No. 194, University of Alberta, Alberta, Canada.